Characterization of silicon oxynitride thin films by x-ray photoelectron spectroscopy

J. R. Shallenberger,[a] D. A. Cole, and S. W. Novak
Evans East, East Windsor, New Jersey 08520

(Received 18 November 1998; accepted 26 April 1999)

There has been a considerable effort in the past decade to incorporate nitrogen into SiO_2 in order to improve the electrical properties of ultrathin (2–10 nm) gate oxides. Process conditions affect the nitrogen concentration, coordination, and depth distribution which, in turn, affect the electrical properties. X-ray photoelectron spectroscopy (XPS) is particularly well suited to obtaining the nitrogen coordination and, to a lesser extent, the nitrogen concentration in thin oxynitride films. To date, at least four different nitrogen coordinations have been reported in the XPS literature, all having the general formula: $N(-Si_xO_yH_z)$, where $x+y+z=3$ and $x \leqslant 3$, $y \leqslant 1$, $z \leqslant 2$. In this article we review the XPS literature and report on a fifth nitrogen coordination, $(O)_2=N-Si$, with a nitrogen $1s$ binding energy of 402.8 ± 0.1 eV. Next nearest neighbor oxygen atoms shifted the $N(-Si)_3$ peak roughly 0.1 eV per oxygen atom. We also discuss results from a novel approach of determining the nitrogen areal density by XPS, the accuracy of which is dependent on the depth distribution of nitrogen. Secondary ion mass spectrometry is used to determine the depth N distribution, while nuclear reaction analysis is used to check the N concentration measured by XPS.
© *1999 American Vacuum Society.* [S0734-2101(99)21904-5]

I. INTRODUCTION

The benefits of incorporating nitrogen into ultrathin SiO_2 films have been studied intensely for more than a decade. A long list of improved electrical properties of oxynitride films compared with SiO_2 has been discovered including: (a) resistance to boron diffusion, (b) immunity to hot carrier effects, (c) higher charge-to-breakdown voltages, and (d) reduced charge trapping. Oxynitride films have been grown directly on Si (using NO or N_2O), or by nitriding SiO_2 films (with N_2, NH_3, NO, etc.) or even by ion implantation of N^+ into SiO_2. Depending on the growth conditions, nitrogen can be piled up at or near the SiO_2–Si interface, uniformly distributed throughout the film, or enriched at the surface. Not surprisingly, the growth conditions also affect the concentration and coordination of nitrogen in the films. A host of analytical techniques, including x-ray photoelectron spectroscopy (XPS) and electron spectroscopy for chemical analysis have been used to try to understand the complex relationship between the deposition conditions, film chemistry, and electrical properties. XPS has primarily been used to correlate chemical shifts in the nitrogen $1s$ spectrum with changes in the N coordination. At least four different coordinations have been isolated in oxynitrides including: $N(-Si)_3$, $(Si-)_2N-H$, $Si-N(-H)_2$ and $(Si-)_2N-O$. It is the goal of this article to investigate the nitrogen concentration and coordination in oxynitride films by XPS. Special attention will be paid to the correlation between depth distribution and concentration. Although depth information is available from XPS (by sample tilting or by HF etch back), secondary ion mass spectrometry (SIMS) is used in these experiments to determine the N distribution. Nuclear reaction analysis (NRA) is used to check the nitrogen areal density measurements.

II. EXPERIMENT

A. Film processing

Several types of oxynitride films were studied. The conditions used to produce the films are outlined in Table I. The type I plasma treatment was done with an Applied Materials Centura rapid thermal processing (RTP) system. The other plasma treatment (type II) consisted of a helicon remote plasma source. Details of the type II process can be found elsewhere.[1]

B. Film characterization

XPS experiments were performed using a Physical Electronics PHI Model 5701 LSci instrument equipped with a monochromatic Al K_α x-ray source ($h\nu = 1486.6$ eV) and a concentric hemispherical analyzer. Charge neutralization was performed using a low energy (<5 eV) electron flood gun. High-resolution spectra were acquired using a pass energy of 11.75 eV and a step size of 0.10 eV. The binding energy axis was calibrated using sputter cleaned Cu foil ($Cu2p_{3/2} = 932.7$ eV, $Cu3p_{3/2} = 75.1$ eV). Peaks were charge referenced to the SiO_2 band in the $Si2p$ spectrum at 103.0 eV. Other authors have charge referenced to the Si^0,[2,3] the Fermi edge,[4] or C–C[5] peaks. The binding energies of the Si^0 peak and the Fermi edge vary with dopant type and concentration making them unreliable choices for charge referencing. The C–C band frequently suffers from differential charging. Also, *in situ* prepared samples do not have an adsorbed carbon layer. All measurements were made at a takeoff angle of 65°, with respect to the sample surface plane. This takeoff angle was chosen, in part, to minimize x-ray photoelectron

[a]Current address: The Pennsylvania State University, 196 Materials Research Institute Bldg., University Park, PA 16802; electronic mail: jxs124@psu.edu

PA108.pdf

TABLE I. Deposition conditions.

Film	Substrate
N_2O (six samples)	Si
$NO–O_2$ mixture	Si
NH_3	SiO_2
N_2 plasma (type I)	SiO_2
N_2 plasma (type II)	SiO_2

diffraction that is known to affect the intensity of the signal from the substrate at specific angles.[6] The Si $2p$ and N $1s$ relative sensitivity factors (RSFs) were determined by analyzing two polymer standards: polydimethyl siloxane $[-(CH_3)_2SiO-]_n$ and polyethylene imine $(-CH_2CH_2NH-)_n$.

SIMS experiments were performed using a Physical Electronics model 6600 quadrupole-based instrument. A 1 keVCs^+ primary ion beam was used and cluster ions (CsO^+, CsN, and $CsSi^+$) detected, are described in more detail elsewhere.[7]

In the NRA measurements the $^{14}N(d,\alpha_{0+1})$ ^{12}C nuclear reaction was induced by 1.1 MeV D^+ with the sample tilted 42° from the beam normal. The N detection limit under these conditions is approximately 4×10^{13} atoms/cm^2. Details have been published elsewhere.[8]

III. RESULTS AND DISCUSSION

A. Nitrogen coordination

A total of six N_2O oxynitrides were prepared; a representative film is presented in Fig. 1(a). The spectra for the N_2O (398.4 eV), NO/O_2 (398.2 eV), and NH_3 (397.9 eV) oxynitrides contain single peaks in the range where $N(-Si)_3$ has been reported. These results agree with previously published studies on NO,[2,3] N_2O,[5,8–12] and NH_3 (Ref. 4) oxynitrides. Bhat *et al.* found an additional N–O containing peak on both 900 °C furnace[9] and 950 °C RTP[10] N_2O oxynitrides. [Note: Only the NH_3 oxynitride was exposed to hydrogen containing species so it is unlikely that there is any significant $(Si-)_2N-H$ present in the other four samples.]

The type II N_2 plasma treated film (398.1 eV) and the remote N_2 plasma treated, type II, film (397.5 eV) contained $N(-Si)_3$ peaks. The type I sample also contained a peak at 399.7 eV characteristic of $O-N(-Si)_2$. The type II oxynitride contained an $O-N(-Si)_2$ peak as well as third peak at 402.8 eV. This unknown peak lies roughly halfway between nitrogen bonded to one oxygen atom, $O-N(-Si)_2$ at 399.7 eV, and nitrogen bonded to three oxygen atoms, NO_3^- at ≈407 eV, and, therefore, is assigned $(O-)_2N-Si$.

An unexpectedly large spread in $N(-Si)_3$ binding energy was observed in this study as well as in the literature.[2–5,9–12] It was initially assumed that the spread in the literature values was due to differences in instrument calibration and/or charge referencing. Since all spectra in our experiments were acquired under identical conditions it raises the possibility that the 0.9 eV spread is due to a chemical, rather than instrumental, effect. Some authors[5,13] interpreted these shifts as

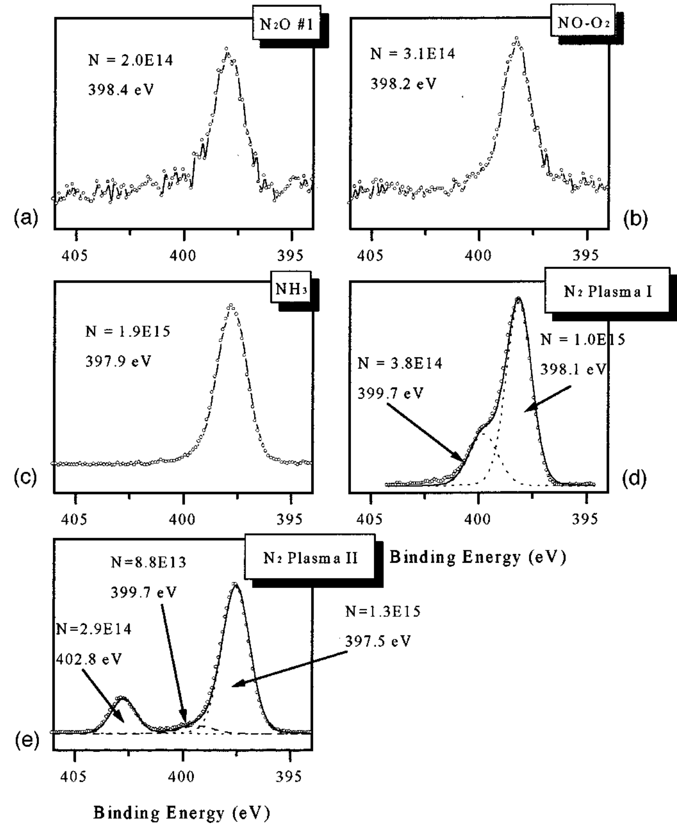

FIG. 1. High-resolution N $1s$ is spectra from oxynitrides grown in (a) N_2O, (b) NO/O_2 mixture, (c) NH_3, (d) N_2RTP plasma treatment type I, and (e) N_2 remote plasma treatment type II. The peaks 397.5–398.4 eV (a)–(e) are due to $N(-Si)_3$. The peak at 399.7 eV (d) and (e) is due to $O-N(-Si)_2$. The peak at 402.8 eV (e) is due to $(O-)_2N-Si$. The areal density of the different nitrogen species is listed for the individual nitrogen coordinations.

evidence for: $N(-Si)_2$ (where ":" is a dangling bond). Bouvet *et al.* interpreted these shifts as evidence for next nearest neighbor oxygen bonds. Careful examination of the correlation between the $N(-Si)_3$ peak position and the areal density

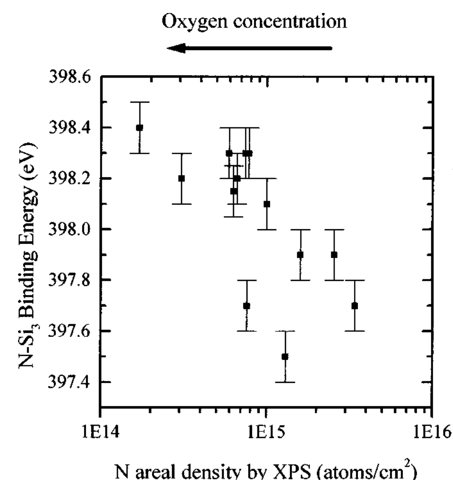

FIG. 2. Plot of the $N(-Si)_3$ nitrogen $1s$ binding energy as a function of N areal density measured by XPS. The shift to higher binding energy at lower N concentration (i.e., higher O concentration) is due to the presence of the more electronegative next nearest neighbor oxygen atoms.

PA108.pdf

TABLE II. Summary of N 1s peak positions, where ``:'' = dangling bond.

Species	N 1s (eV)	Reference
$N(-Si)_3$	397.4–398.4	This study and 2–5, 9–12
$(Si-)_2N-H$	398.0	4
$Si-N(-H)_2$	398.6	4
$(Si-)_2N-O$	399.7–401.0	This study and 3, 9–11
$Si-N(-O)_2$	402.8	This study

of nitrogen supports the latter explanation. Figure 2 reveals a shift toward lower binding energy with increasing nitrogen concentration. A lower nitrogen concentration (i.e., higher oxygen concentration) leads to an increased number of next nearest neighbor oxygen atoms. The more electronegative oxygen atoms shift the $N(-Si)_3$ binding energy as much as 0.9 eV. The maximum number of next nearest neighbor oxygen atoms is 9 for an average shift of 0.1 eV per next nearest neighbor oxygen. (This assumes, of course, that the samples studied here actually spanned the entire 0–9 range of allowable next nearest neighbor oxygen atoms.) Samples with higher nitrogen concentration have a lower probability of having next nearest neighbor oxygen atoms and, hence, appear more like Si_3N_4. A summary of reported N 1s positions from this and other oxynitride studies is listed in Table II.

B. Nitrogen concentration

Quantification of XPS data from homogeneous (with depth) samples is commonly done by integrating peak areas and applying RSFs. Oxynitride samples create special quantification problems because the samples are generally inhomogeneous within the ≈10 nm sampling depth. Signal is detected from the SiON layer (which itself may have a nonuniform N distribution), as well as from the Si^0 substrate and an adsorbed surface organic layer. In light of this problem quantification has largely been left to SIMS,[14–17] NRA,[8,18,19] and medium energy ion scattering (MEIS).[3,20–22]

Recently we showed that the areal density of boron and arsenic present in ultrathin SiO_2 layers could be determined using XPS.[23] A similar approach can be applied to oxynitrides to determine the nitrogen areal density. The approach requires that two assumptions be made about the sample: (1) nitrogen is only present in the oxynitride layer, and (2) the nitrogen concentration is constant throughout the oxide layer. The former case is nearly always true, but the latter case is frequently false. The procedure involves measuring the relative amounts of nitrogen, $(N)_{rel}$, and oxidized silicon, $(Si^{4+})_{rel}$. The relative oxygen concentration is calculated using Eq. (1) rather than being directly measured, to avoid counting oxygen associated with the organic layer

$$(O)_{rel}=2(Si^{4+})_{rel}-0.75(N)_{rel}. \quad (1)$$

Carbon from the adsorbed organic overlayer and silicon from the substrate are ignored. The 0.75 term removes silicon that is bonded to nitrogen, i.e., for simplicity it is assumed that N is present as Si_3N_4. The atom fraction of nitrogen present in the oxynitride layer is then given by

$$(N)_{rel}=\frac{(N)_{rel}}{(N)_{rel}+(Si^{4+})_{rel}+(O)_{rel}}. \quad (2)$$

Finally, the N areal density (in atoms/cm^2) can be calculated as

$$N(\text{atoms/cm}^2)=(N)_{atom}N_{SiO_2}t_{ox}, \quad (3)$$

where N_{SiO_2} is the atom density of SiO_2 (6.6×10^{22} atoms/cm^3) and t_{ax} is the oxide thickness.[24] The oxide thickness was calculated using the following equation:

$$t_{ox}=\lambda_{SiO_2}\sin\theta\ln\left[\left(\frac{I_{Si}^{\infty}}{I_{SiO_2}^{\infty}}\frac{I_{SiO_2}^{exp}}{I_{Si}^{exp}}\right)+1\right], \quad (4)$$

where, λ_{SiO_2} is the attenuation length of the Si 2p photoelectrons in SiO_2, θ is the takeoff angle, I_{Si}^{∞} and $I_{SiO_2}^{\infty}$ are the Si 2p intensities from ``infinitely'' thick Si^0 and SiO_2, respectively. $I_{SiO_2}^{exp}$ and I_{Si}^{exp} are the Si intensities from the unknown film determined by curve fitting the Si 2p spectrum into component peaks. The attenuation length ($\lambda_{SiO_2}=3.4$ nm) was determined by analyzing a series of SiO_2 films previously characterized by high resolution cross section transmission electron microscopy (TEM), Rutherford backscattering (RBS), and ellipsometry. The determination of I_{Si}^{∞} and $I_{SiO_2}^{\infty}$ was done by analyzing two different standard samples: a 5% HF etched Si (100) surface and a 85-nm-thick thermal SiO_2 film. Both were lightly sputtered with 3 keV Ar^+ to remove adsorbed organic species (and the native oxide and fluoride on the HF etched Si sample). The $I_{Si}^{\infty}/I_{SiO_2}^{\infty}$ value measured in our experiments (after accounting for implanted argon and readsorbed gases) was 1.20.

Figure 3 shows the Si 2p spectrum from a typical oxynitride sample. All Si 2p spectra were fit as a series of doublets split by 0.60 eV, reflecting the spin orbit splitting of the 2p shell. Elemental silicon $2p_{3/2}$ peak widths varied from 0.48 to 0.52 eV, while the oxidized Si peak widths were 1.20–1.35 eV wide. Similar to Mitchell *et al.*,[25] a small peak (in this case, a doublet) 0.3 eV from the main Si^0 peak was added to introduce asymmetry to this peak. There was excellent agreement between the thickness determined using Eq. (4) with the thickness determined by TEM, ellipsometry, and RBS. To gauge the precision of the XPS measurement the 3.6 nm film (as measured by TEM), was analyzed several times over a seven month time period. The average oxide thickness was 3.59 ± 0.07 nm ($1\sigma=2.0\%$). The precision in measuring the nitrogen atom fraction [Eq. (2)] was checked on the same 3.6 nm oxynitride and found to be 3.0%, for an overall precision of the XPS measurement of 5.0%. The detection limit of this approach is approximately $1E13$ atoms/cm^2.

The areal density of the different coordinations of nitrogen as measured by XPS is shown on the individual N 1s spectra in Fig. 1. Although growth conditions varied considerably it is clear that NH_3 and N_2 plasma treatments result in higher nitrogen concentrations than either NO or N_2O treatments. Figure 4 compares nitrogen areal density measured by

PA108.pdf

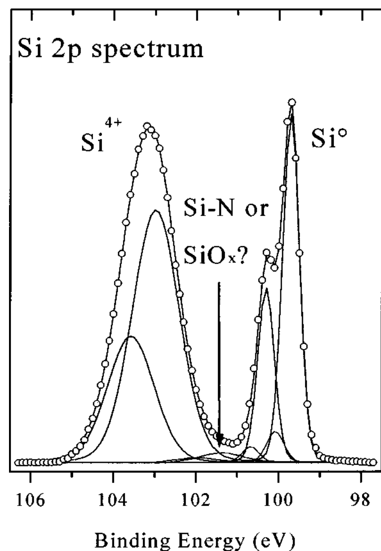

FIG. 3. Si $2p$ spectrum from a 3.6 nm oxynitride film fit into component peaks to determine the experimental $I_{SiO_2}^{exp}$ (64.0%) and I_{Si}^{exp} (36.0%). A small peak has been added at 101.8 eV where Si_3N_4 is expected.

XPS and NRA. There is good agreement for four of the seven samples, but the remaining three samples disagree by more than the combined estimated error ($\approx$12%) of the techniques. A clue to this unexpectedly large error may be found in the SIMS depth profiles.

C. Nitrogen distribution

Although the N $1s$ spectra for the N_2O, NO/O_2, and NH_3 oxynitrides contained a single $N(-Si)_3$ peak, the SIMS depth profiles revealed dramatic differences in depth distribution (Fig. 5). Nearly all the nitrogen in the N_2O #2 oxynitride is piled up at the SiO_2–Si interface 3.5 nm below the surface. A similar pileup has been observed in many previous studies on N_2O oxynitrides. Carr and Buhrman[13] found interfacial nitrogen enrichment in N_2O samples grown by rapid thermal oxidation, although they found furnace N_2O films had more uniform nitrogen distribution. Since on average the nitrogen photoelectrons are originating from deeper in the material than the Si^{4+} photoelectrons, the nitrogen electrons are disproportionately attenuated resulting in an underestimate of the true nitrogen concentration. The sample grown in a NO/O_2 mixture exhibited a more uniform N distribution within the oxide layer, consistent with recent MEIS studies on films grown in pure NO[3] and a NO/N_2 mixture.[22] The result was in better agreement with NRA. Finally, the N_2O #1 oxynitride has nitrogen located near the outer surface and the result is an overestimate of the nitrogen concentration by XPS because of disproportionate attenuation of the Si^{4+} photoelectrons relative to the N photoelectrons.

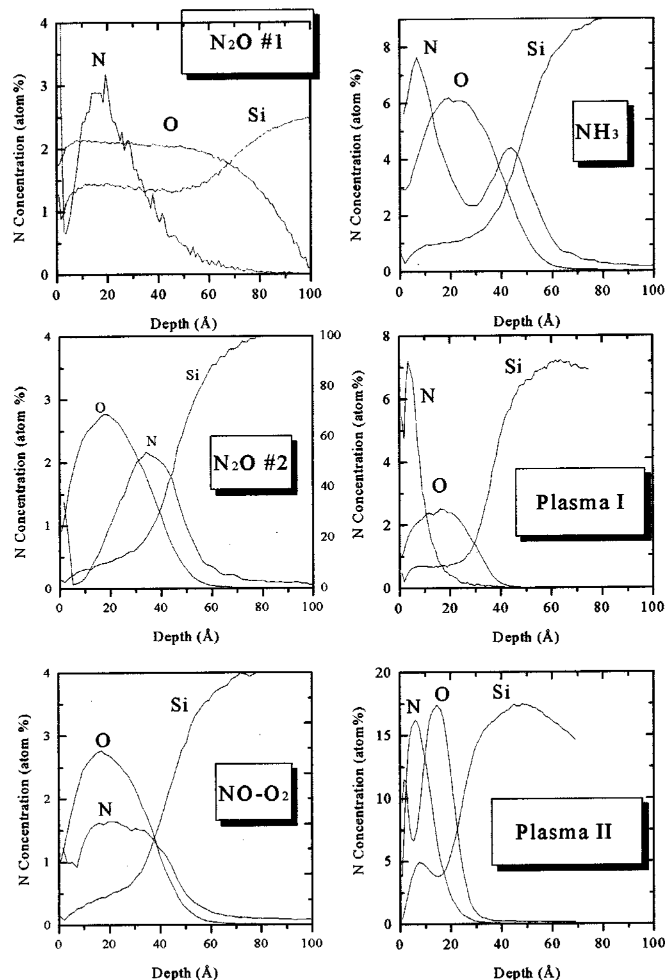

FIG. 5. SIMS depth profiles showing nitrogen in-depth distribution.

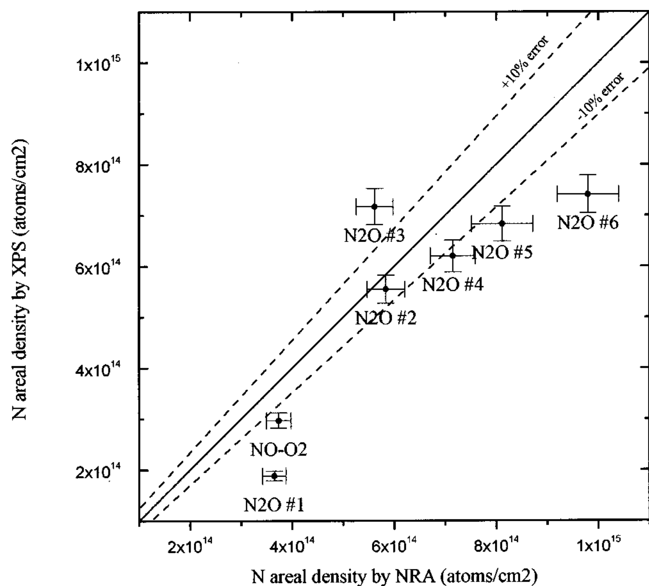

FIG. 4. Nitrogen concentration determined by XPS (ordinate) vs the concentration as determined by NRA (abscissa). Sample N_2O #1 contained a surface-rich N layer, while sample N_2O #2 had a subsurface-rich nitrogen layer. Samples falling on or near the dotted line tended to have nitrogen uniformly distributed throughout the oxide.

The NH_3 treated oxynitride film contained both a surface and interfacial N peak, consistent with other studies.[26–28] The plasma treated oxynitride films both contained thin (<2 nm) surface-rich nitrogen layers on top of a SiO_2 layer. NRA

PA108.pdf

measurements were not performed on the NH_3 or plasma processed oxynitrides.

The accuracy of the XPS areal density measurement is dependent on the depth distribution. The accuracy is also somewhat dependent on the oxynitride layer thickness; thicker inhomogeneous layers will tend to have a larger underestimation of N on buried layers and a larger overestimation of N on surface layers. However, as oxynitride film thickness decreases to <3.0 nm the magnitude of this error should also decrease.

IV. CONCLUSIONS

XPS was used to determine the nitrogen coordination in ultrathin (<6 nm) silicon oxynitrides processed a variety of ways. Films formed by N_2O, NO/O_2, and NH_3 contained a single nitrogen peak identified as $N(-Si)_3$. Small shifts to higher binding energy in the $N(-Si)_3$ peak position may be the result of next nearest neighbor oxygen atoms bonded to silicon. A new nitrogen species, $(O-)_2N-Si$, present at 402.8 ± 0.1 eV in the N $1s$ spectrum, was observed in an oxynitride formed by remote N_2 plasma nitridation. There was good agreement in nitrogen areal density with NRA for samples that had nitrogen uniformly present throughout the oxide layer. When N was preferentially located at the SiO_2-Si interface the nitrogen concentration was underestimated due to attenuation of the signal from the overlying oxide layer. Conversely, when nitrogen was located near the surface, the nitrogen concentration was overestimated by XPS.

ACKNOWLEDGMENTS

The authors would like to thank Dr. Gary Xing of Applied Materials, Dr. Sunil Hattangady of Texas Instruments, and Dr. Marty Green of Bell Labs for providing the films used in this study. Thanks also to Dr. Guiti R. Massoumi of The University of Western Ontario for the NRA measurements.

[1]R. Kraft, T. P. Schneider, W. W. Dostalik, and S. Hattangady, J. Vac. Sci. Technol. B **15**, 967 (1997).
[2]R. I. Hegde, B. Maiti, R. S. Rai, K. G. Reid, and P. J. Tobin, J. Electrochem. Soc. **145**, L13 (1998).
[3]H. C. Lu, E. P. Gusev, T. Gustafsson, E. Garfunkel, M. L. Green, D. Brasen, and L. C. Feldman, Appl. Phys. Lett. **69**, 2713 (1996).
[4]J. L. Bischoff, F. Lutz, D. Bolmont, and L. Kuber, Surf. Sci. **251/252**, 170 (1991).
[5]S. R. Kaluri and D. W. Hess, Appl. Phys. Lett. **69**, 1053 (1996).
[6]J. M. Hill, D. G. Royce, C. S. Fadley, L. F. Wagner, and F. J. Grunthaner, Chem. Phys. Lett. **44**, 225 (1976).
[7]M. R. Frost and C. W. Magee, Appl. Surf. Sci. **104/105**, 379 (1996).
[8]H. T. Tang, W. N. Lennard, M. Zinke-Allmang, I. V. Mitchell, L. C. Feldman, M. L. Green, and D. Brasen, Appl. Phys. Lett. **64**, 3473 (1994).
[9]M. Bhat, J. Ahn, D. L. Kwong, M. Arendt, and J. M. White, Appl. Phys. Lett. **64**, 2116 (1994).
[10]M. Bhat, G. W. Yoon, J. Kim, D. L. Kwong, M. Arendt, and J. M. White, Appl. Phys. Lett. **64**, 1168 (1994).
[11]D. Bouvet, P. A. Clivaz, M. Dutoit, C. Coluzza, J. Almeida, G. Margaritonondo, and F. Pio, J. Appl. Phys. **79**, 7114 (1996).
[12]W. Ting, H. Hwang, J. Lee, and D. L. Kwong, Appl. Phys. Lett. **57**, 2808 (1990).
[13]E. C. Carr and R. A. Buhrman, Appl. Phys. Lett. **63**, 54 (1993).
[14]H. Hwang, W. Ting, B. Maiti, D-L Kwong, and J. Lee, Appl. Phys. Lett. **57**, 1010 (1990).
[15]Y. Okada, P. J. Tobin, R. I. Hegde, J. Liao, and P. Rushbrook, Appl. Phys. Lett. **61**, 3163 (1992).
[16]G. Weidner and D. Kruger, Appl. Phys. Lett. **62**, 294 (1993).
[17]N. S. Saks, D. I. Ma, and W. B. Fowler, Appl. Phys. Lett. **67**, 374 (1995).
[18]M. L. Green, D. Brasen, K. W. Evans-Lutterodt, L. C. Feldman, K. Krisch, W. Lennard, H.-T. Tang, L. Manchanda, and M.-T. Tang, Appl. Phys. Lett. **65**, 848 (1994).
[19]I. J. R. Baumvol, J.-J. Ganem, L. G. Gosset, I. Trimaille, and S. Rigo, Appl. Phys. Lett. **72**, 2999 (1998).
[20]M. Copel, R. M. Tromp, H.-J. Timme, K. Penner, and T. Nakao, J. Vac. Sci. Technol. A **14**, 462 (1996).
[21]H. C. Lu, E. P. Gusev, T. Gustafsson, and E. Garfunkel, J. Appl. Phys. **81**, 6992 (1997).
[22]E. P. Gusev, H. C. Lu, T. Gustafsson, E. Garfunkel, M. L. Green, and D. Brasen, J. Appl. Phys. **82**, 896 (1997).
[23]J. R. Shallenberger, D. A. Cole, D. F. Downey, S. Falk, and Z. Zhao, Proceedings of the XIIth International Conference on Ion Implantation Technology, Kyoto, Japan, 1998 (in press).
[24]T. Watanabe, A. Ichikawa, M. Sakuraba, T. Matsuura, and J. Murota, J. Electrochem. Soc. **145**, 4252 (1998).
[25]D. F. Mitchell, K. B. Clark, J. A. Bardwell, W. N. Leonard, G. R. Massoumi, and I. V. Mitchell, Surf. Interface Anal. **21**, 44 (1994).
[26]Y. Yoriume, J. Vac. Sci. Technol. B **1**, 67 (1983).
[27]R. P. Vasquez, M. H. Hecht, F. J. Grunthaner, and M. L. Naiman, Appl. Phys. Lett. **44**, 969 (1984).
[28]M. M. Moslehi, K. C. Saraswat, and S. C. Shatas, Appl. Phys. Lett. **47**, 1113 (1985).